

# THE GAS TINY FLOW MEASUREMENT INSTRUMENTATION

Milan Adámek, Petr Neumann, Martin Pospíšilík  
Tomas Bata University in Zlín  
Department of Security Engineering, Faculty of Applied Informatics  
Nad Stráněmi 4511, 76005, Zlín  
Czech Republic  
E-mail: adamek@fai.utb.cz

## KEYWORDS

flow measurement, calorimetric sensor, time – of – flight, heating power, mass and heat transfer, modelling, Femlab, flow tube, flow range

## ABSTRACT

The paper presents the design and experimental experience with the gas flow measurement instrument for the range of (5 – 25) *ml/hr*. The aimed application area is in a biochemical laboratory for the study of reaction kinetic of sediments decomposition in waste water. The time – of – flight type of sensor with one upstream and one downstream temperature sensor has been chosen for the study. We explain the basic operation principles of the tiny flow measurement and the sensor structure. In the numerical model paragraph, we are describing the basic configuration model and the modelling results. As the three – dimensional simulation would be very time consuming process, we have simplified the simulation for only two – dimensional task. The presented diagrams are derived for different gases (air, nitrogen, carbon oxide and chlorine) and sensor tube materials, namely steel, copper, and plexi-glass. We present also the experimental set – up including the design and sensor parameters. The paragraph with experimental results and discussion on them illustrates the good correspondence with expected values. The paper concludes with the employment of designed gas flowmeter in the biochemical laboratory.

## INTRODUCTION

The accurate measurement and control of tiny liquid flows in the amount of nanoliters up to milliliters per minute is becoming more and more important for a lot of applications in the life science. In some applications, such as process control in precise semiconductor manufacturing, chemical and pharmaceutical industries and biochemical engineering, miniaturized liquid flow sensors are more and more encountered. Most of them operate on the method of thermal transport and are fabricated from a silicon crystal by using micromachining technology.

The thermal devices for flow measurement may be grouped in two different classes. The first class groups thermal mass flowmeters that are measuring the effect

of the flowing fluid on a hot body (the increase of heating power with constant heater temperature, the decrease of heater temperature with constant heating power). They are usually called hot – wire, hot – film sensors or hot – element sensors. The resistive element is used both as heater and as sensor simultaneously. The temperature can be obtained from its electrical resistance. The second class group thermal mass flowmeters that measure the displacement of temperature profile around the heater which is modulated by the fluid flow. These sensors are called calorimetric sensors. The special type of thermal mass flowmeters in the class mentioned above is thermal mass flowmeter that measure the heat pulse passage time over a known distance. They are usually called time – of – flight sensors [1].

Many of the microflow sensors use a thermopile as a temperature sensor; however, the thermoelectric coefficient of the standard elements used in the integrated circuit is smaller than that of conventional thermocouples. Thus, a resulting output signal may be very small which requires amplifiers integrated directly into the sensor [2].

Up to now, very few of nowadays commercially offered flow sensors are equipped with the features mentioned above. One of possible method of liquid flow measuring is presented in this paper. The properties of a time – of – flight sensor are studied. The FEMLAB program was used for the study of flow sensor properties.

## SENSOR STRUCTURE AND BASIC OPERATING PRINCIPLE

The flow sensor consists of a heater and one or more downstream temperature sensors, as shown in the Figure 1a. The heater is activated by current pulses. The transport of the generated heat is a combination of diffusion and forced convection. The resulting temperature field can be detected by temperature sensors located downstream. The detected temperature output signal of the temperature sensor is a function of time and flow velocity. The sensor output is the time difference between the starting point of the generated heat pulse and the point in time at which a maximum temperature at the downstream sensor is reached, Figure 1b. This type of sensor has the same constraints as the intrusive type of calorimetric sensors: corrosion,

erosion and leakage [3]. Since the signal processing needs some time to measure the time difference, this sensor type is not suitable for dynamic measurement. On the other side, the advantage of this type of flow sensor is the independence on the fluid temperature in the wider flow range. The influence of fluid properties on the mass flow sensor output is described in [4].

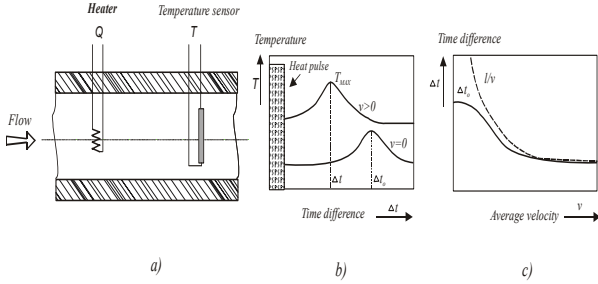


Figure 1: Time – of – flight sensor: a) principle; b) temperature at the downstream sensor; c) sensor characteristic

The transport of the heat generated in a line source through a fluid follows the energy equation [5]

$$\frac{\partial T}{\partial t} + u\nabla T = \left( \frac{\lambda}{\rho c} \right) \nabla^2 T + \frac{q}{\rho c} \quad (1)$$

where  $T$  is the temperature,  $c$  is the specific heat at the constant pressure,  $\rho$  is the density,  $\lambda$  is the thermal conductivity,  $q$  is the amount of heat per unit of volume and time. The analytical solution of this differential equation for a pulse signal with input strength  $q$  ( $Wm^{-1}$ ) is given in [5] as

$$T(x, y, t) = \left( \frac{q}{4\pi\lambda t} \right) \exp \left\{ - \frac{[(x-ut)^2]}{4at} \right\} \quad (2)$$

where  $a$  denotes the thermal diffusivity.

## NUMERICAL MODEL

In the presented work, the properties of the time – of – flight sensor were investigated using commercially available program FEMLAB. Femlab is an interactive environment for modelling and solving problems based on partial differential equations. This program applies the finite element method (FEM) for the PDEs system solving [6].

The simulated time – of – flight sensor is a multiphysics model which means that it involves more than one kind of physics. In this case, there are Navier-Stokes equations from fluid dynamics together with a heat transfer equation that is essentially a convection-diffusion equation. There are three unknown field variables: the velocity  $u$ , the pressure  $p$  and the

temperature  $T$ . They all are interrelated through bidirectional multiphysics couplings.

The equations are:

- Conservation of mass: continuity equation

$$\frac{\partial \rho}{\partial t} + \nabla(\rho u) = 0 \quad (3)$$

- Conservation of momentum: Navier – Stokes equation

$$\rho \frac{\partial u}{\partial t} + \rho(u \cdot \nabla)u = -\nabla p + \eta \nabla^2 u + F \quad (4)$$

- Conservation of energy: energy equation

$$\frac{\partial T}{\partial t} + v\nabla T = \left( \frac{\lambda}{\rho c} \right) \nabla^2 T + \frac{q}{\rho c} \quad (5)$$

where  $\eta$  is the dynamic viscosity.

## BASIC CONFIGURATION

Since a typical full three – dimensional simulation of the sensor requires in excess of  $10^5$  cells and therefore several computational days, it was decided to investigate several configurations in two dimensions at first.

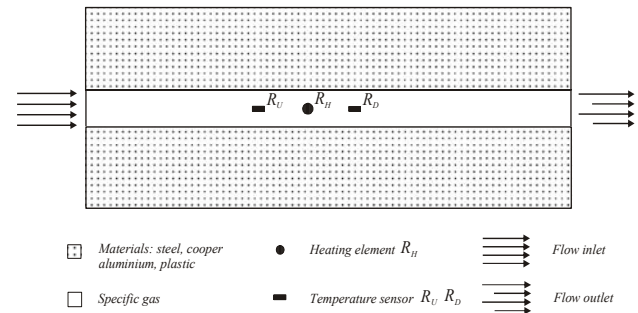


Figure 2: Basic configuration studied

The two dimensional configuration assumed in the presented work is illustrated in Figure 2.

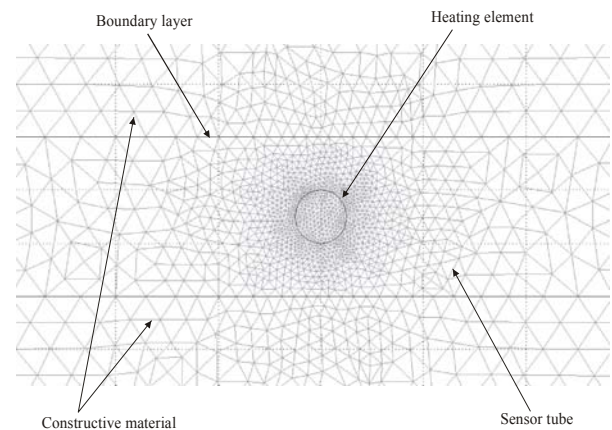


Figure 3: Partial view of the computational grid for the basic configuration

A structured computational grid consisting of more than 23000 cells was generated. Close attention was paid to the grid resolution in critical areas such as boundary layers and the surroundings of the heater. A part of the grid for the basic configuration is displayed in Figure 3. Even in the two dimensional case, the convergence to a correct solution required several computational hours on a 2,2 GHz PC.

The properties of the time – of – flight sensor were investigated at the relatively very low flow rates. In table 1, there are some inlet gas velocities  $v$  used in the sensor model and the corresponding flow rate  $Q$  (the inner diameter of sensor tube is 1 mm).

Table 1. Inlet speeds of fluent gas.

$v(mm\ s^{-1})$	$Q(ml\ h^{-1})$
1,76	5
3,54	10
5,29	15
7,08	20
8,82	25

The effects of the sensor output tube constructive material were investigated at the same time, too. The boundary conditions of the sensor model and the heat coefficients can be found in Figure 4. The transport of the heat from the sensor tube to the ambient is expressed as:

$$h = \frac{1}{\frac{1}{\alpha_1} + \frac{\delta}{k} + \frac{1}{\alpha_2}} \quad (6)$$

where  $h$  is the heat transfer coefficient,  $\alpha_1$  is the coefficient of heat transfer by convection (from sensor tube to constructive material),  $k$  is the thermal conductivity of the constructive material,  $\alpha_2$  is the coefficient of heat transfer by convection (from constructive material to ambient) and  $\delta$  is the thickness of the constructive material.

The coefficient of heat transfer by convection from sensor tube to constructive material  $\alpha_1$  was derived (*forced convection*) with the help of Nusselt number expressed as [7]:

$$Nu = 1,86 \left( Pe \frac{d}{l} \right)^{\frac{1}{3}} \left( \frac{\eta}{\eta_w} \right)^{0,14} \quad (7)$$

where  $Pe$  is Peclet number,  $\eta$  is dynamic viscosity,  $\eta_w$  is dynamic viscosity at wall temperature,  $l$  is length of heat transfer surface and  $d$  is inner diameter of the heat exchanger shell. The coefficient of heat transfer by convection from constructive material to ambient  $\alpha_2$  was calculated (*natural convection*) with the help of Nusselt number expressed as [7]:

$$Nu = 1,18 \cdot (Gr \cdot Pr)^{1/8} \quad (8)$$

where  $Gr$  is Grashof number and  $Pr$  is Prandtl number.

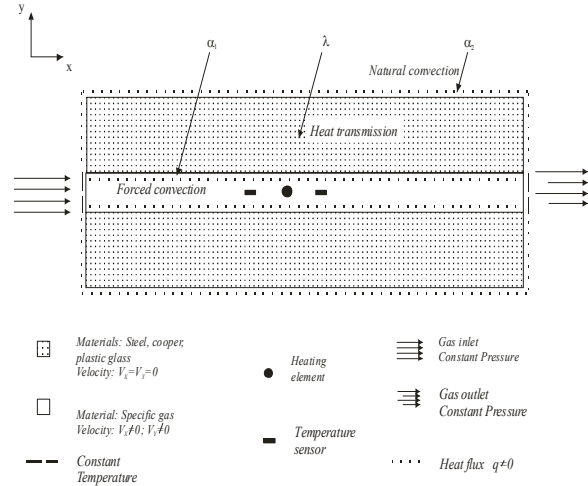


Figure 4: Boundary settings in the model of the time – of – flight sensor

The properties of the time – of – flight sensor were simulated and verified for different constructive materials and different flowing gases, Table 2 and Table 3.

Table 2. Physical constants of the applied gases.

Flowing gases	Density $\rho (kg \cdot m^{-3})$	Heat capacity $c (J \cdot kg^{-1} \cdot K^{-1})$	Thermal conductivity $\lambda (W \cdot m^{-1} \cdot K^{-1})$	Dynamic viscosity $\eta (Pa \cdot s)$
$CO_2$	1,9768	825	0,0159	$15,6 \cdot 10^{-6}$
$N_2$	1,2505	1043	0,0255	$18,6 \cdot 10^{-6}$
$Cl$	3,1221	486	0,0082	$13,4 \cdot 10^{-6}$
<i>air</i>	1,1641	1010	0,0252	$18,3 \cdot 10^{-6}$

Table 3. Physical constants of the applied constructive materials.

Constructive materials	Density $\rho (kg \cdot m^{-3})$	Heat capacity $c (J \cdot kg^{-1} \cdot K^{-1})$	Thermal conductivity $k (W \cdot m^{-1} \cdot K^{-1})$
<i>copper</i>	8930	383	386
<i>steel</i>	7850	482	50
<i>plexi-glass</i>	1185	1460	0,18

## MODELLING RESULTS

The functionality  $\Delta T$  (Figure 1) on the flow rate  $Q$  at downstream sensor RD are shown in Figure 5, 6, 7; the temperature  $T_{MAX}$  was measured in the distance of 1,25mm from the heater (in the middle of temperature sensor) in the models. The mentioned temperature functionalities at the upstream sensor  $R_U$  are depicted in Figure 8, 9, 10. Figure 11 shows the functionality of time difference  $\Delta t$  on the flow velocity  $u$ . As can be seen in Figure 1,  $\Delta t$  is the difference between the time of the heat pulse and the time of  $T_{MAX}$ .

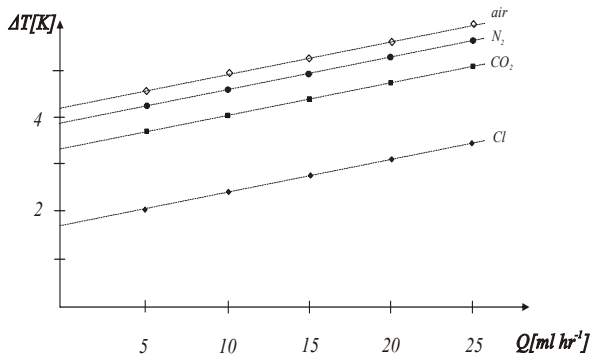


Figure 5: The functionality  $\Delta T$  on flow rate  $Q$  at downstream sensor RD, constructive material plexi – glass

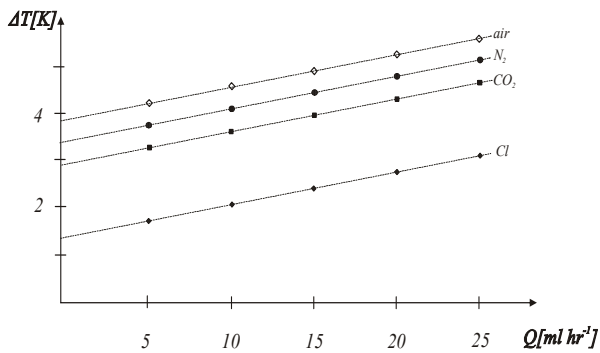


Figure 6: The functionality  $\Delta T$  on flow rate  $Q$  at downstream sensor RR, constructive material steel

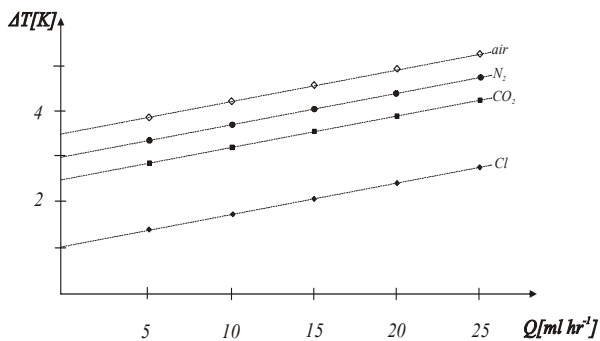


Figure 7: The functionality  $\Delta T$  on flow rate  $Q$  at downstream sensor RD, constructive material cooper

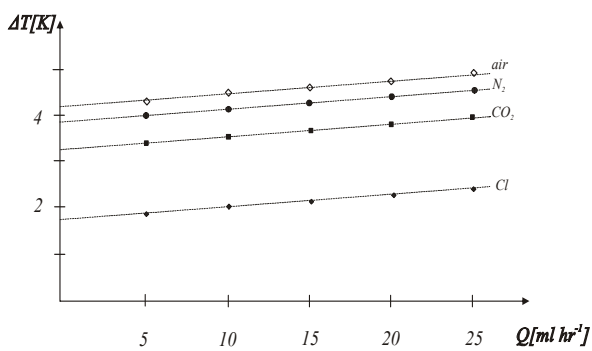


Figure 8: The functionality  $\Delta T$  on flow rate  $Q$  at upstream sensor R<sub>U</sub>, constructive material plexi – glass

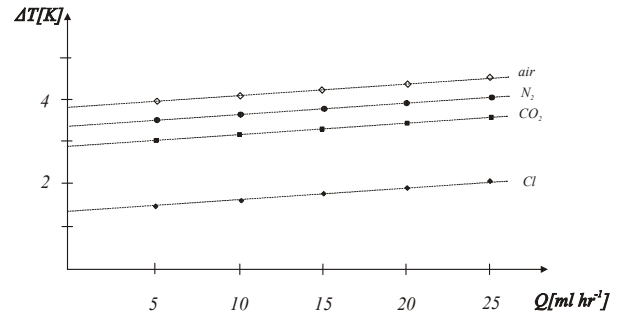


Figure 9: The functionality  $\Delta T$  on flow rate  $Q$  at upstream sensor R<sub>U</sub>, constructive material steel

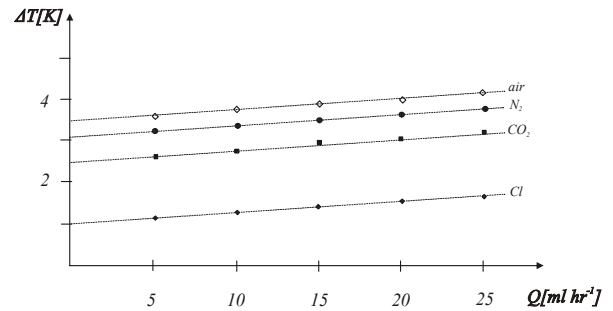


Figure 10: The functionality  $\Delta T$  on flow rate  $Q$  at upstream sensor R<sub>U</sub>, constructive material cooper

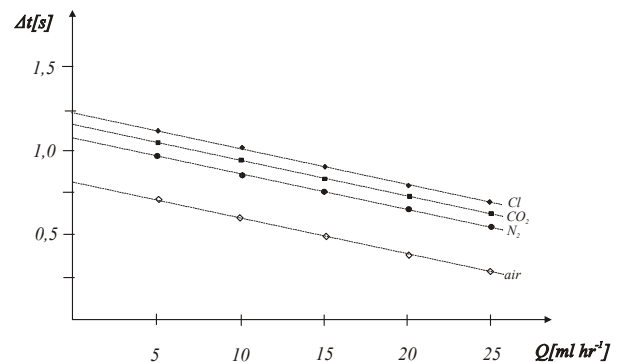


Figure 11: The functionality  $\Delta t$  on flow rate  $Q$  at upstream and downstream sensor, constructive material cooper

## EXPERIMENTAL SET – UP

The main goal of this work was to develop the flowmeter with the measured flow range of (5 – 25) ml/hr. However, the mechanical and electrical design was important as well because of practical realisation.

## FLOW TUBE

The modelling results had set the inspiration data for a construction variant of the flow tube. Several gas flow sensors have been built, with flow tubes made out of stainless steel and cooper, and with internal diameters varying between 0,5 and 1,5 mm. The corresponding internal volumes of the flow sensor tubes are 9,8  $\mu$ l and 39,3  $\mu$ l, respectively.

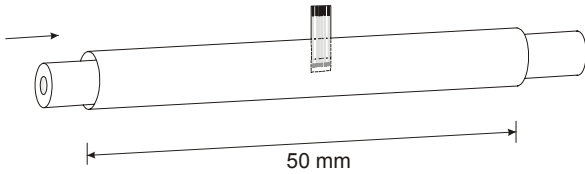


Figure 12: The flow tube

### SENSOR ELEMENT

There was used the product of Swiss company Flow – Sens, FS2 as sensor element. The FS2 is the result of continuous development of IST AG quality products. This new element consists of three temperature depending platinum – resistors, all deposited on one substrate. The low-ohm resistor with a small area is used as a heater, whereas the two high-ohm resistors on the right and on the left side are for measuring the mass flow and the direction. As a result of the little thermal mass, this flow sensor has fast heating and cooling response times. Technical specifications of the mentioned sensor are [8]:

- Response time:  $< 0.5$  s
- Temperature range:  $-20 \dots + 60$  °C
- Temperature sensitivity:  $< 0.1$  %/K
- Permissible pressure: 100 bar (depending on the sensors incorporation, higher pressure upon requests)
- Permissible humidity: 0 ... 95% rH (no condensation)
- Electrical connection flexible circuit, compatible with ZIF connector
- Heater:  $R_H(0^\circ\text{C}) = 25 \Omega$
- Measuring elements:  $R_L, R_R(0^\circ\text{C}) = 250 \Omega$
- Sensor dimensions:  $5 \times 3.5 \times 0.15$  mm
- Substrate material: ceramic  $0.15$ mm

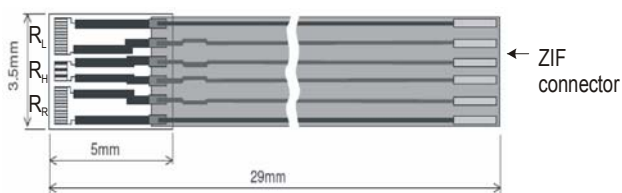


Figure 13: Sensor element

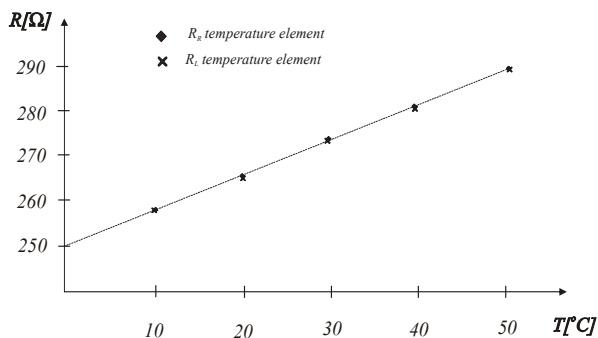


Figure 14: Static characteristic of sensor element

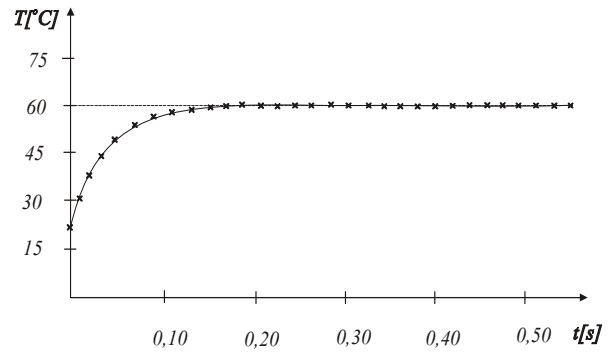


Figure 15: Dynamic characteristic of sensor element

### ELECTRONIC CIRCUIT

The mass flow controller implementation was built of two sensors working according to the time – of – flight measurement principle. Both temperature sensors need their own specific electronic circuitry which is based upon a Wheatstone bridge configuration. The electronic circuitry converts the output signals, namely  $\Delta T$  of each temperature sensor into an output voltage.

The items to be specified in Figure 16 are:

- $U_{IH}$  supply voltage of heater
- $U_{CC}$  supply voltage of Wheatstone bridge
- $U_{OL}$  output voltage of upstream temperature sensor
- $U_{OR}$  output sensor of downstream temperature sensor

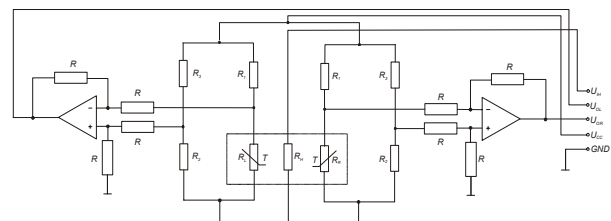


Figure 16: Electronic circuitry

The heater is activated periodically; the pulse heating is used in flow tube according to the time – of – flight measurement principle. A length of the heating pulses is  $0.2$  s, a period of heating pulses is  $3$  s.

### RESULTS AND DISCUSSION

The output signal of the flow sensors was measured for flow ranges varying between  $5 - 25$  ml/hr in the downstream and upstream sensor. The mass flow controller was used for measurements of the dynamic behaviour. The following two variations in set point were stepwise performed:

- $0\% \Rightarrow 100\% \Rightarrow 0\%$
- $20\% \Rightarrow 40\% \Rightarrow 60\% \Rightarrow 80\% \Rightarrow 100\%$

The resulting response of the mass flow sensor was measured with a digital oscilloscope.

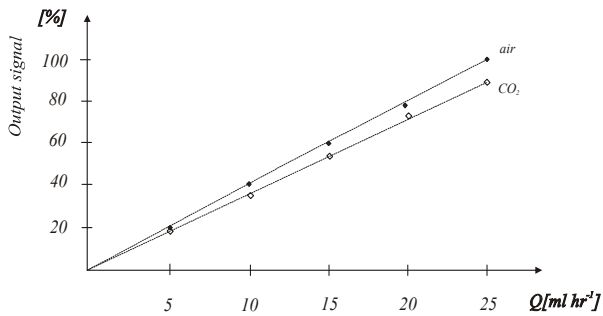


Figure 17: Measurement results obtained with gas flow sensor (downstream sensor) with flow range  $25 \text{ ml/h} \cong 100\%$  according to the time – of – flight measurement principle and its working range; the flow tube is made of stainless steel and have an internal diameter of  $1 \text{ mm}$ .

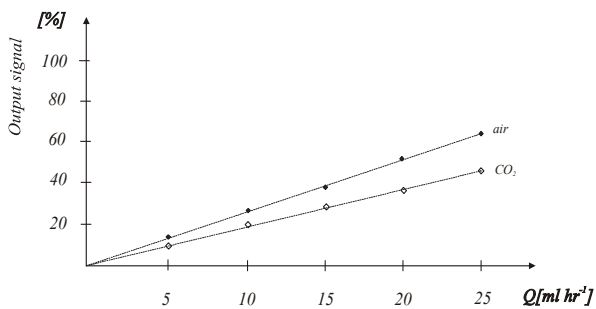


Figure 18: Measurement results obtained with gas flow sensor (upstream sensor) with flow range  $25 \text{ ml/h} \cong 100\%$  according to the time – of – flight measurement principle and its working range; the flow tube is made of stainless steel and have an internal diameter of  $1 \text{ mm}$ .

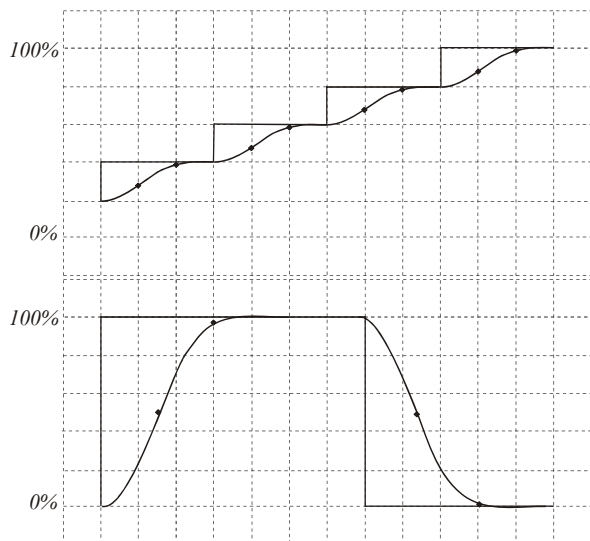


Figure 19: Measured response times of a gas flow sensor adjusted for air:  $25 \text{ ml/h} \cong 5 \text{ V}$ ; the X - axis represents the time [s] with  $2 \text{ s} / \text{div.}$ , the Y - axis displays the output voltage [V] with  $1 \text{ V} / \text{div.}$ ; the flow tube is made of stainless steel and has an internal diameter of  $1 \text{ mm}$ ; the sensor is working according to the time – of – flight measurement principle.

The measured curves, as displayed in Figures 17 through 19, correspond well with the theoretically expected values as calculated with equations (3), (4) and (5). However, some deviations between theory and measurements have occurred. They can be explained as follows:

- real dimensions, real temperatures and pressures differed from the values used in the calculations.
- not all boundary conditions for equations (3), (4) and (5) were fully fulfilled, so that the heat transfer had a somewhat different behaviour than expected.

The measured response times, as shown in Figure 19, are all within the value of  $t_{98\%} = 6 \text{ s}$ .

The above mentioned flow sensor structures and operating principles have the following innovative features and advantages:

- The flow sensor comprises a short straight flow tube, with an internal diameter varying between  $0,5$  and  $1,5 \text{ mm}$ , thus having a small internal volume, varying between  $9,8 \mu\text{l}$  and  $39,3 \mu\text{l}$ .
- The measurable flow range is  $5$  to  $25 \text{ ml/h}$ , the response time  $t_{98\%}$  is  $6$  second.
- The measurable flow range can easily be adjusted by varying the internal diameter, material and wall thickness of the flow tube.
- The material of the flow tube can be either stainless steel or cooper or plastic glass; other materials may also prove to be feasible.
- The length of the flow sensor tube is the same for all flow ranges. This enables a modular set-up and exchangeability of instruments.

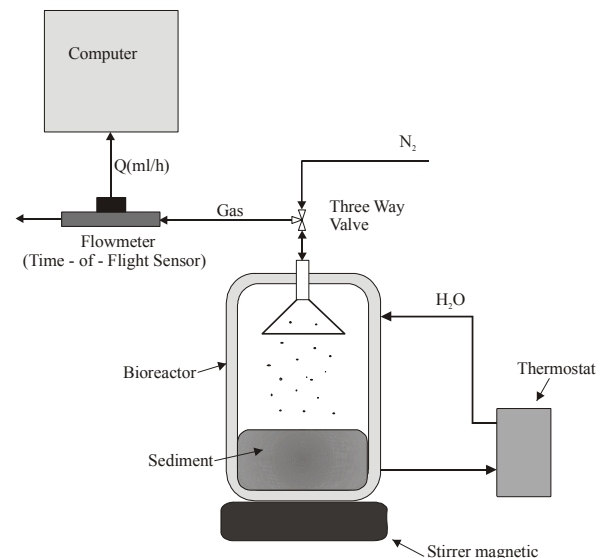


Figure 20: Employment of designed flowmeter in a biochemical laboratory

## CONCLUSIONS

In this article, the measurement method of small gas flow called as time – of – flight method is presented. The measurement results exhibit that the designed flow

sensor is acceptable for slow processes with reference to response time of  $t_{98\%} = 6 \text{ s}$ .

The designed flowmeter has been used in a biochemical laboratory for study of reaction kinetic of sediments decomposition in the waste water; the decomposition takes about 36 hours. A basic set-up is illustrated in Figure 20 which demonstrates the employment of designed flowmeter in a biochemical laboratory.

## REFERENCES

- Webster, J.: *The measurement, instrumentation and sensors*, Springer, 1999.
- Fraden, J.: *Handbook of modern sensors*, Springer, 2004.
- Lammerink, T., Dijkstra, F., Z. Housek and J. Kuijk.: "Intelligent gas/mixture flow sensor", *J Sensors and Actuators*, Volume A 37/38, p. 45-50, 1995.
- Bonne, U.: "Fully compensated flow microsensor for electronic gas metering", In Proc. *Int. Gas Research Conf. 859*, 1992.
- Kuijk, J., Lammerink, T., Bree, H., Elwenspoek, M., and Fluitman, L.: "Multiparameter detection in fluid flow", *J Sensors and Actuators*, Volume A 46/47, p. 380-4, 1995.
- Perry, R. and Chilton, C.: *Chemical engineers handbook*, McGraw – Hill, 1973.

## AUTHOR BIOGRAPHIES



**MILAN ADÁMEK** graduated in 1990 from the Olomouc Palacky University, Czech Republic. He received his Ph.D. degree in Technical Cybernetics at Tomas Bata University in Zlin in 2002. From 1997 to 2008 he worked as senior lecturer at the Faculty of Technology, Brno University of Technology. From 2008 he has been working as an associate professor at the Department of Electronic and Measurement, Faculty of Applied Informatics of the Tomas Bata University in Zlín, Czech Republic. Current work covers following areas: power lines, camera system, sensors. His e-mail address is: [adamek@fai.utb.cz](mailto:adamek@fai.utb.cz).



**Petr NEUMANN** has been graduated from the Brno Technical University in Electronic Technology in 1974. He has acquired the industrial experience in the field of medical electronics and quality management as R&D engineer. He received his Ph.D. degree in Technical Cybernetics at Tomas Bata University in Zlin in 2001. He has been lecturing and working in the university research area since 1994. He was engaged in the SMT technology training, equipment installation and servicing more than 10 years between 1997 and 2009. He is currently working as a senior lecturer at Tomas Bata University in Zlin. His research work is aimed at

the electronic component authenticity analysis and failure diagnosis. His e-mail address is: [neumann@fai.utb.cz](mailto:neumann@fai.utb.cz)



**MARTIN POSPÍŠILÍK** graduated in 2008 from Czech Technical University in Prague, Czech Republic, in Microelectronics. Having received his Ph.D. degree in Engineering Informatics at Tomas Bata University in 2013, he became an assistant and researcher at the Department of Computer and Communication Systems of Faculty of Applied Informatics of the Tomas Bata University in Zlín, Czech Republic. His current research covers the following topics: electromagnetic compatibility, shielding effectiveness of materials for avionics, design of construction of electrical circuits and testing of electrical devices considering the security of communication. The security issues are investigated in cooperation with Escola Superior de Tecnologia e Gestão, Beja, Portugal. His e-mail address is: [pospisilik@fai.utb.cz](mailto:pospisilik@fai.utb.cz).